Int J Adv Manuf Technol (2017) 90:2741–2749
DOI 10.1007/s00170-016-9564-6

ORIGINAL ARTICLE

Influence of process parameters on abrasive particle motion characteristics in abrasive water jet descaling

Xuecheng Zhang [1] · Cunlong Zhou [1] · Lianyun Jiang [1] · Rui Guo [1]

Received: 14 April 2016 / Accepted: 6 October 2016 / Published online: 21 October 2016

Abstract The motion characteristics of particles play important roles on the quality and efficiency in abrasive water jet machining. In this paper, the abrasive water jet flow field is simulated by computational fluid dynamics (CFD). It is found that when the jet is continuous, there will form a static pressure zone on the surface of the workpiece, where pressure is high and fluid velocity is low. As the existence of static pressure zone, the velocity and motion direction of particles will be changed. Particles with different diameters and densities are compared when they are piercing through the static pressure zone. It can be found that in particles with greater diameter, the motion direction will be hard to be changed and the impact velocity will be higher. Particles with higher density, the motion direction will be also hard to be changed and the impact velocity will be higher. The influence of the radial position has also been considered. Closer to the jet axis, the impact velocity will be higher and the change quantity of motion direction will be smaller. It also can be seen that with the increasing of diameter or density, the influence of radial position on motion direction and impact velocity decreases.

Keywords Motion characteristics of particles · Abrasive particle water jet · CFD · Diameter of particles · Density of particles

✉ Cunlong Zhou
zcunlong@tyust.edu.cn

[1] Shanxi Provincial Key Laboratory of Metallurgical Device Design Theory and Technology, Taiyuan University of Science and Technology, Taiyuan 030024, China

1 Introduction

Abrasive water jet machining removes material or changes micromorphology by liquid and abrasive particles with high speed. As it has many advantages, such as strong adaptability, low residual stress, no thermal effect, and low processing cost, it has been widely used in cutting and cleaning industry [1, 2]. At present, the domestic and foreign scholars are studying or have used abrasive water jet descaling to replace acid pickling descaling, which is an important pretreatment process of strip cold rolling [3, 4]. Abrasive water jet descaling is similar with abrasive water jet flow cleaning. It utilizes the abrasive water jet to eliminate the metal oxide attached to metal strip surface. There are some special requirements for abrasive water jet descaling, such as uniform descaling, surface roughness can be controlled, high efficiency, and abrasive recharging.

Many parameters can influence the efficiency and quality of abrasive water jet machining. They are classified as hydraulic, mixing/nozzle, cutting, and abrasive parameters. Among these parameters, abrasive particle size and their distribution influence the target parameters [5–11], as the abrasive particles will disintegrate during the acceleration and focusing process, and also when machining. The cost of abrasives has restricted usage of abrasive water jet technology in cutting applications. Therefore, many researchers are studying the recycling of the abrasives to make the technology more economical [12, 13]. Aydin G et al. [14] compared the surface roughness experiment results of granites, which machining with different diameter abrasive particles, and concluded that the small abrasive particles produced lower surface roughness. Liu H et al. [15] studied abrasive water jet characteristics by computational fluid dynamics (CFD) simulation, and concluded that smaller diameter particles decelerate more rapidly than larger particles. However, research on the motion characteristics of abrasive particles with variable diameter and density has received little attention.

The motion characteristics of abrasive particles play important roles in the quality and efficiency of the abrasive water jet machining. In the process, water and abrasive particles are jetted from the nozzle to impact the surface of the work piece, and the motion characteristics of abrasive particle are affected by the flow field and the parameters of particles. The influence of abrasive particle size, particle density, and particle radial distribution on the particle motion is studied and analyzed by the finite element method. The results are compared with the experimental results of other researchers. They have certain directive significance to the thorough research and the production practice of the related problems.

2 Impact model of particles on workpiece

Abrasive water jet machining is the effect of many abrasive particles. In order to grasp the law of its processing, a single abrasive particle is chosen as the research object. As shown in Fig. 1, the rigid ball (abrasive particle) with a radius of R impacts the workpiece and makes it to produce elastic deformation. The contact angle between the ball and the workpiece is φ, the normal force is σ, and tangential force is τ. According to the Hertz contact theory, the particle impact depth λ can be expressed as follows [16]:

$$\lambda=\left[\frac{9}{16}\frac{P^2}{R}\left(\frac{1-\nu_1^2}{E_1}+\frac{1-\nu_2^2}{E_2}\right)^2\right]^{1/3} \tag{1}$$

where E_1 is elastic modulus of the abrasive particle (GPa); ν_1 is Poisson's ratio of the abrasive particle; E_2 is the elastic modulus of the workpiece (GPa); and ν_2 is Poisson's ratio of the workpiece.

The impact pressure corresponding to the Eq. (1) can be obtained as follows:

$$P=\frac{4}{3}\left(\frac{1-\nu_1^2}{E_1}+\frac{1-\nu_2^2}{E_2}\right)^{-1}R^{1/2}\lambda^{3/2}. \tag{2}$$

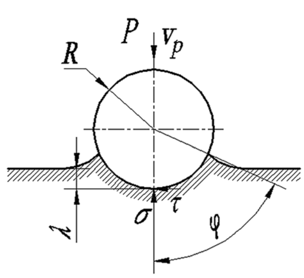

Fig. 1 Sketch map of particle vertical impact workpiece

Considering the stress wave motion equation is given as:

$$mv_pv_p=-Pv_p \tag{3}$$

where m is the mass of particle (kg); v_p is the velocity of particle (m/s); and ρ_p is the density of particle (kg/m^3).

Integral on both sides of Eq. (3), then, the particle impact depth λ can be expressed as:

$$\lambda=\left[\frac{5\pi}{4}\rho_p\left(\frac{1-\nu_1^2}{E_1}+\frac{1-\nu_2^2}{E_2}\right)\right]^{2/5}R\cdot v_p^{4/5} \tag{4}$$

Equation (4) substituted into Eq. (2), the corresponding impact pressure can be expressed as:

$$P=\frac{4}{3}\left(\frac{5\pi}{4}\rho_pv_p\right)^{3/5}\left(\frac{1-\nu_1^2}{E_1}+\frac{1-\nu_2^2}{E_2}\right)^{-2/5}R^2. \tag{5}$$

As shown in Fig. 2, the abrasive particles impact the workpiece at any angle α. The angle is called impact angle. The particle speed v_p can be decomposed into vertical velocity $v_p\sin\alpha$, which is perpendicular to the surface of the workpiece, and horizontal velocity $v_p\cos\alpha$, which is parallel to the surface of the workpiece.

When $v_p\sin\alpha$ is substituted into Eq. (4), the general form equation of particle impact depth can be expressed as:

$$\lambda=\left[\frac{5\pi}{4}\rho_p\left(\frac{1-\nu_1^2}{E_1}+\frac{1-\nu_2^2}{E_2}\right)\right]^{2/5}R\left(v_p\sin a\right)^{4/5}. \tag{6}$$

The corresponding vertical impact force (along Y axis) can be expressed as:

$$P_V=\frac{4}{3}\left(\frac{5\pi}{4}\rho_p\right)^{3/5}\left(\frac{1-\nu_1^2}{E_1}+\frac{1-\nu_2^2}{E_2}\right)^{-2/5}R^2\left(v_p\sin\alpha\right)^{6/5}. \tag{7}$$

The corresponding horizontal impact force (along X axis) can be expressed as:

$$P_H=\frac{4}{3}\left(\frac{5\pi}{4}\rho_p\right)^{3/5}\left(\frac{1-\nu_1^2}{E_1}+\frac{1-\nu_2^2}{E_2}\right)^{-2/5}R^2\left(v_p\cos\alpha\right)^{6/5}. \tag{8}$$

According to the theory of Bitter [17, 18], the material removal method can be divided into deformation wear and cutting wear. The impact depth is influence by vertical impact force P_V, while the plow length is influence by horizontal

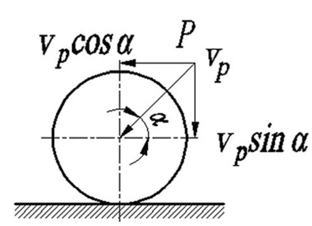

Fig. 2 Sketch map of particle impact target workpiece with angle α

impact force P_H. By Eq. (6)~(8), it can be seen that the velocity, size, and density of particles play important roles on the impact depth and impact force.

3 Model and boundary conditions

The finite element method is widely used in the jet research, and the accuracy of the result was validated by the experiment when using the turbulence model [19].

3.1 Finite element mathematical model

3.1.1 Discrete phase model

In order to simplify the abrasive particle flow field model, the following assumptions are made in the abrasive water jet machining:

(1) The initial phases in the flow field are air and water, and abrasive particles are added into the water phase in the form of discrete phase.
(2) Abrasive particles are assumed to be spherical and equal in size.
(3) The abrasive water jet has less solid concentration, assuming that the movement between abrasive particles does not interfere with each other, and the particle motion does not affect the movement of the fluid.

The tracks of discrete phase particles in FLUENT are obtained by integrating the differential equation of forces of particles in the Lagrangian coordinate system. In the form of Cartesian coordinate system, the force balance equation (particle inertia is a variety of forces acting on the particle) of particles can be expressed as (taking x direction for an example) [20]:

$$\frac{dv_p}{dt} = F_D\left(v - v_p\right) + \frac{g_x\left(\rho_p - \rho\right)}{\rho_p} + F_x \tag{9}$$

$$F_D = \frac{18\mu}{\rho_p d_p^2}\frac{C_D Re}{24} \tag{10}$$

$$Re = \frac{\rho d_p\left|v_p - v\right|}{\mu} \tag{11}$$

$$C_D = \alpha_1 + \frac{\alpha_2}{Re} + \frac{\alpha_3}{Re^2} \tag{12}$$

where v is the velocity of fluid (m/s); $F_D(v - v_p)$ is the drag force per unit particle mass (N); g_x is the gravity acceleration in the x direction (m/s^2); ρ is the density of fluid (kg/m^3); F_x is other forces in the x direction (including the Basset force, Magnus force, and Saffman's lift force, etc.) (N); μ is the dynamic viscosity of fluid (Pa s); d_p is the diameter of the particle of abrasive (m); Re is the relative Reynolds number; C_D is the drag coefficient; and α_1, α_2, and α_3 are constants that apply over several ranges of Re given by Morsi and Alexander.

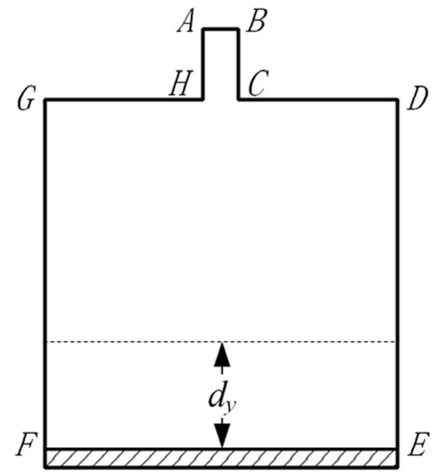

Fig. 3 Abrasive water jet flow field model

3.2 Model establishment and boundary setting

A cross section of the abrasive water jet flow field is taken as the research object, and it is simplified as a two-dimensional model for finite element calculation to improve the calculation speed, as shown in Fig. 3. The abrasive water jet flow field is the field where water and abrasive are being jetted from the nozzle, interacting with the air, and impacting on the workpiece. Model of the nozzle is *ABCH*. The diameter (*AB*, *HC*) of the nozzle is 1 mm, and the length (*AH*, *BC*) is 2 mm; the model of the flow field is *GDEF*; the length of *GF* and *DE* is 10 mm, and the length of *GD* and *EF* is 10 mm. The model is calculated by FLUENT. The volume of fluid (VOF) model is set as the multiphase flow model, and the discrete phase model (DPM) is used at the same time. Standard k-ε model is chosen as the turbulence model, and the steady-state model is used for calculating.

Boundary conditions are set as follows: AB is chosen as the pressure inlet, the value is 100 MPa, and the reference pressure value is 101,325 Pa; HG, GF, CD, and DE are set as the pressure outlet, the value is 0 Pa, and the reference pressure value is 101,325 Pa; AH, and BC are set as the wall of the nozzle, which are used no slip wall as the boundary condition; and FE is set as the surface of the workpiece, which is used no slip and rigid wall as the boundary condition. Other parameter initial settings are shown in Table 1.

Table 1 Model parameters used in simulation

Density of water (kg/m^3)	Viscosity of water (Pa s)	Density of particle (kg/m^3)	Diameter of particle (mm)
998.2	0.001	2600	0.18

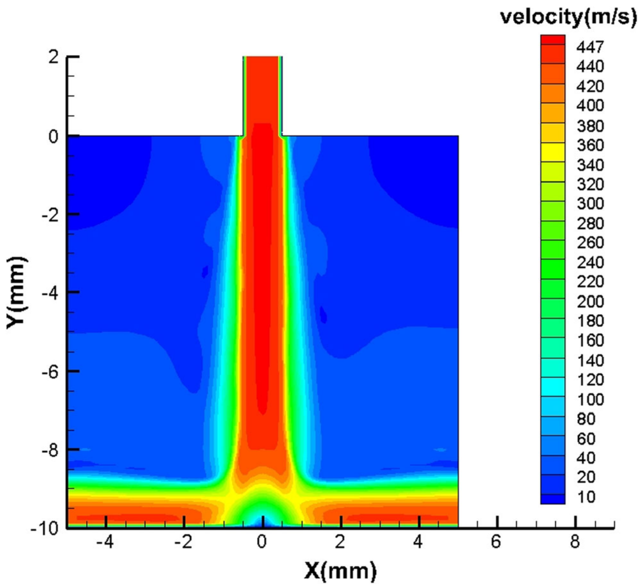

Fig. 4 Velocity contour of the whole flow field

4 Calculation results and analysis

4.1 The characteristics of the particle flow field

When the inlet pressure is 100 MPa, and other initial and boundary conditions are according to the above settings, the calculation results are obtained by finite element method, as shown in Fig. 4.

In the situation of continuous jet, when the jet fluid is impacting on the surface of the workpiece, the velocity of fluid is decreasing suddenly, and the fluid flow is blocked; the compression wave is generated in the fluid. There will form a region on the liquid-solid contact interface, where pressure is very high and fluid velocity is very low or even stay, which is called the static pressure zone, as shown in Fig. 4.

Table 2 Maximum pressure at the sampling point near the jet axis

d_y (mm)	0.2	0.4	0.6	0.8	1.0
P (MPa)	95.6	87.8	75.3	60.1	44.0

The pressure data of the flow field near the surface of the workpiece are summarized, as shown in Fig. 5, where d_y is the distance from the sampling point to the surface of the workpiece in the Y axis direction, as shown in Fig. 3.

From Fig. 5, it can be seen that the pressure values show normal distribution. The values at the jet axis are the maximum, and the pressure values gradually decrease with the increasing of the distance from the axis. When the distance is three times of the diameter of the nozzle, the pressure values drop to zero. At the same time, it can be seen that the pressure decreases with the increasing of the distance from workpiece.

The maximum pressure of the sampling points near the jet axis is listed in Table 2.

From Table 2, it can be seen that the rate of pressure decline is increasing with the d_y. The static pressure zone mainly concentrates in the jet center, and the pressure is very high.

The velocity data of the flow field near the surface of the workpiece are summarized to analyze the characteristic of the velocity change in the vicinity of the static pressure zone, as shown in Fig. 6.

From Fig. 6, it can be seen that the velocity values show normal distribution. The velocity decreases with the decreasing of the distance from the workpiece in the Y axis direction. And the velocity increases with the increasing of the distance from the jet axis. When the distance reaches two times of the diameter of the jet, the velocity is reaching the maximum. When the distance d_y is 0.8 mm, the velocity is substantially unchanging with the increasing of the distance from the jet axis. Associating with Fig. 4, it can be found that it is out of the core area of the jet. When the distance d_y is 1.0 mm, the

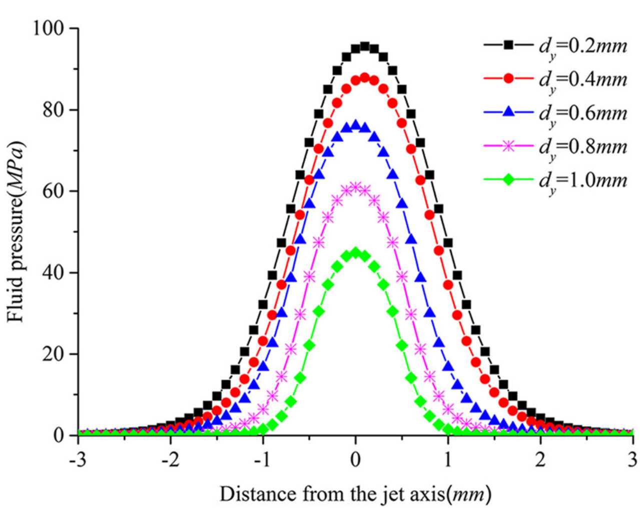

Fig. 5 Pressure distribution in the vicinity of static pressure zone

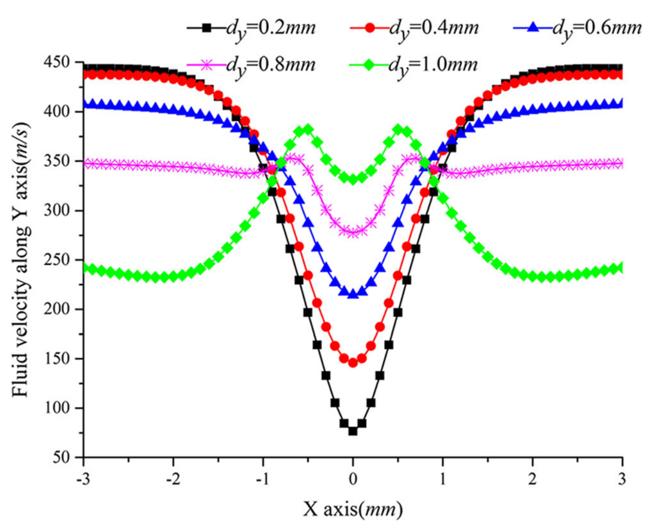

Fig. 6 Velocity distribution in the vicinity of the static pressure zone

velocity is declining when it has a certain distance from the jet axis. It can be found that it is located in the region of strong interaction between fluid and air, and the velocity loss is very great.

To sum up, the pressure of the static pressure zone is very high, and the velocity is very low; the fluid at the center of the jet is like a protective cover on the surface of the workpiece, and it is like an obstruction to the fluid and abrasive particles in the post-order jet. At the same time, it is shown that the high pressure of pure water jet relies on the pressure of the static pressure zone. When the pressure value reaches to the compressive strength limit of the processed materials, and the material of the workpiece will be removed, then it needs higher pressure than the abrasive water jet machining.

4.2 The motion characteristics of particles

4.2.1 The influence of particle diameter

Particles with diameter 180 μm are often be used in abrasive water cutting, and they can realize high material removal rates. Simultaneously, particles will disintegrate during the acceleration and focusing process, and also when machining, there are will be different diameters in the jet flow. And particles with a diameter of 5 or 20 μm are often be used in abrasive water polishing, and they can realize fine surface finish. Abrasive water descaling needs both fine surface finish and good material removal efficiency. In order to decide to reuse or discard, the particle motion characteristic of particles with different diameters should be obtain. So the study of the motion characteristics of particles with the diameters 5, 20, and 180 μm has important significance for particle choice.

The diameter of particle is set with different values (5, 20, and 180 μm) in the DPM model to study the influence of particle diameter on the motion track of particle. The initial velocities of particles are set to 0 m/s. The tracks of particles are obtained by CFD, as shown in Fig. 7.

From Fig. 7, it can be seen that when the diameter of particle is 5 μm, the motion direction of abrasive particles has great deflection when approaching the surface of the workpiece, and there are almost no particles that can penetrate the static pressure zone and impact on the center of the static pressure zone, while abrasive particles in the edge of the jet have no impact on the workpiece and move along the direction parallel to the workpiece. With the increasing of the particles diameter, the deflection angles will decrease. There are more abrasive particles that can penetrate the static pressure zone and impact on the surface of the workpiece.

In order to further study the effect of static pressure zone on abrasive particles with different diameters, the correlation data of the abrasive particles with the distance 0.05 mm away from the jet axis are compared and analyzed, as shown in Figs. 8 and 9, where d_p is the diameter of particles.

From Fig. 8, it can be seen that particles are moving along the *Y* axis before they enter the static pressure zone. Once entering the zone, the motion direction of particles will be changed, which can be measured by relative deflection angle of particles. Deflection angle values are related to the diameter of particles. When particles impact on the workpiece, particles with a diameter of 5 μm have the relative deflection angle of 88°, particles with a diameter of 20 μm have the relative deflection angle of 28.8°, and particles with diameter of 180 μm have the relative deflection angle of 6.7°. In conclusion, the deflection angles decrease with the increasing diameters of the particles.

From Fig. 9, it can be seen that when particles enter the flow field from the inlet, as the initial velocities of particles are 0 m/s, the velocity of the fluid is larger than particles and particles have been accelerated. Particles with smaller mass are accelerated more easily. Particles with the diameter of 5 μm are the first to reach the stable velocity, 447 m/s. Particles with the diameter of 20 μm are the second to reach the stable velocity, 441 m/s. Particles with diameter of 180 μm have been accelerated continually before they enter the static pressure zone, and the maximum velocity is 395 m/s. When entering the static pressure zone, the velocity of fluid is smaller than particles and particles have been decelerated. Particles of smaller diameter are decelerated more easily. When particles impact on the workpiece, particles with a diameter of 5 μm have the velocity along *Y* axis of 12.9 m/s, particles with a diameter of 20 μm have the velocity of 75 m/s, and particles with a diameter of 180 μm have the velocity of 166 m/s. In conclusion, the impact velocities increase with the increasing diameter of particles.

It concluded that particles with greater diameter are more difficult to be accelerated, as they have bigger mass. But they could obtain more kinetic energy from the liquid. After

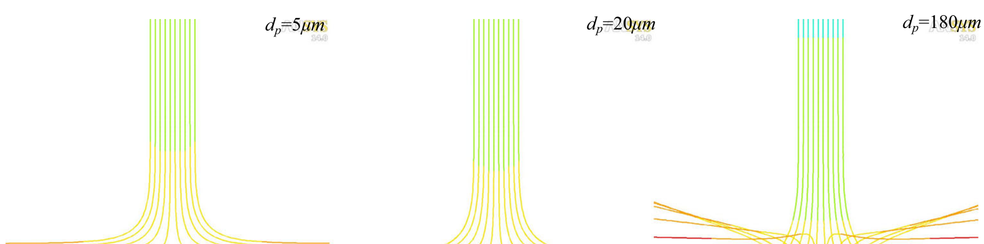

Fig. 7 Tracks of particles with different diameters in the flow field

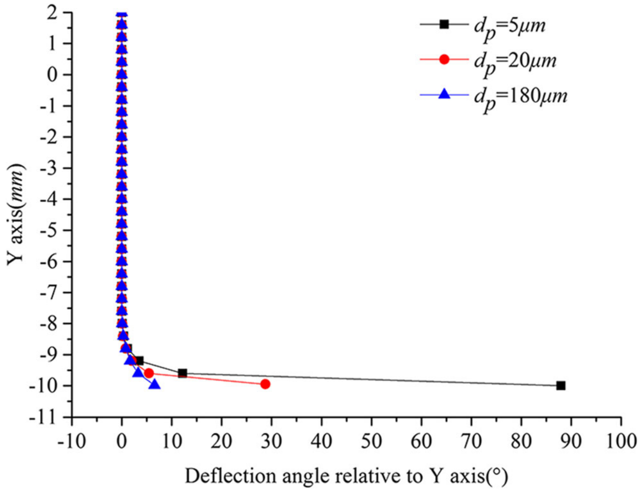

Fig. 8 Deflection angle relative to *Y* axis of particles with different diameters

through the static pressure zone, they also have more vertical impact velocity value. According to Eq. (6), it can be concluded that the greater particles will have more material impact depth. So the greater particles will have more material removal rates. It is consistent with the experimental results of Wang R. J. [21]. Simultaneously, in particles with greater diameter, their motion direction will be more difficult to be changed.

The impact velocities of different diameter particles along *Y* axis are shown in Fig. 10.

The jet center has the highest velocity in free jet, so the velocities of particles near the jet center will be the highest. As the effect of the static pressure zone, the particles near the jet center will departure the jet axis with a distance and impact on the workpiece with the highest velocity, as shown in Fig. 10. The velocity distribution of particles with diameter of 5 μm is coinciding with the profile on the workpiece after machining, and the removed material in the center of the machining zone is the lowest (almost zero). And only the distance from the jet center of 0.05 mm can impact the workpiece. So a distance from the jet axis will have more material removal rates. The profile through the spot center is approximately a "W" shape [22]. When the diameter of particles is 20 μm, the relative deflection angle will decrease. With the increasing of distance from the jet axis along *X* axis, the impact velocity decreases. Particles near the center will have the highest velocity, as the particles near the jet center have small deflection angle. There will be more material removal rates in the jet center as the deformation wear. With the distance from the jet axis increasing, the deflection angles increase. There is an existing cutting wear at the same time. As the conclusions of Finnie I [23], the cutting wear will have maximum material removal rates, when the impact angle is about 18°. So the spot center and a distance from the jet axis will have more material removal rates. It is consistent with experimental results of Zhang et al. [16]. The profile through the spot center is approximately a "VVV" shape. When the diameter of particles is 180 μm, the relative deflection angle is small, the impact area is more concentrated, and the material removal is mainly focus on the center. The profile of the spot center is a "V" shape [24].

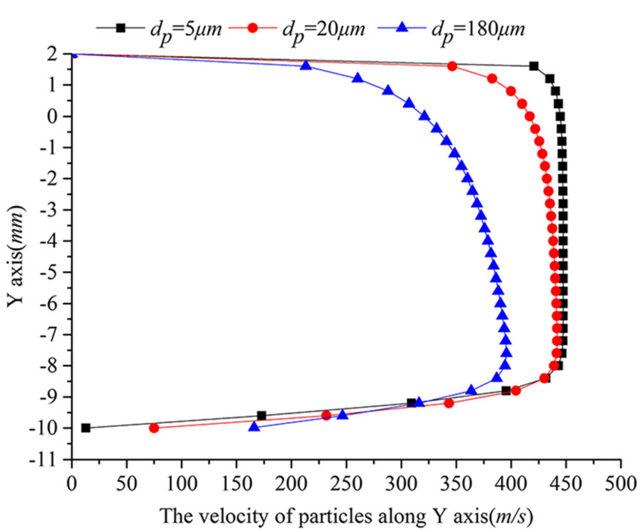

Fig. 9 The velocity along *Y* axis of particles with different diameters

4.2.2 The influence of particle density

There are many kinds of abrasive particles with different densities that are used in practice. The density of particles is an important parameter, the influence of which should be intensive study. The results of the influence of the density of particle on the motion characteristics of the particles are obtained by CFD, when the jet pressure is 100 MPa and the particle diameter is 180 μm. The initial velocity of particles is set to 0 m/s. The data of the particle density (ρ_p) of 2600, 4200, and 7850 kg/m^3 are compared and analyzed, as shown in Fig. 11.

From Fig. 11, it can be seen that with the increasing of the particle density, the motion direction of the particles in the

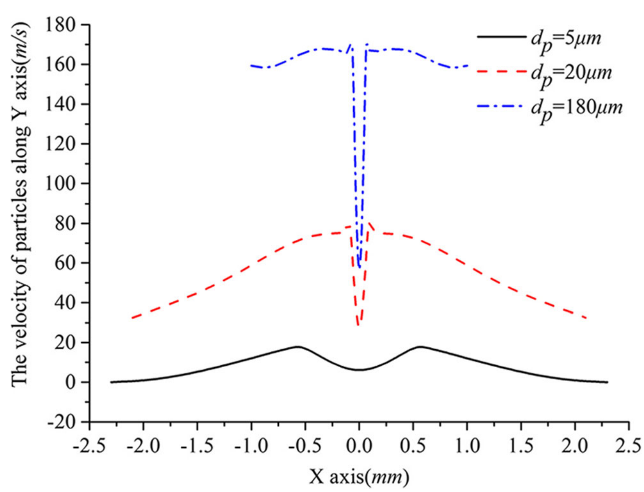

Fig. 10 The distribution of velocities of particles along *Y* axis on the workpiece

Fig. 11 Tracks of particles with different densities in the flow field

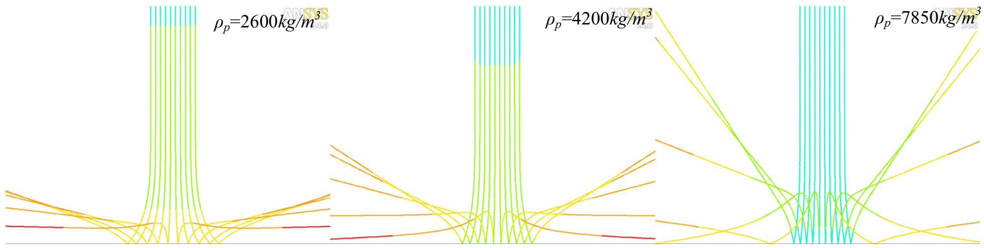

vicinity of the static pressure zone is more difficult to be changed, and the jet influenced area decreases and the jet beam of particles is becoming more concentrated. The data of the three densities of particles in the radial distance from the jet axis of 0.05 mm are compared and analyzed, as shown in Figs. 12 and 13.

From Fig. 12, it can be seen that particles are moving along *Y* axis before they enter the static pressure zone. Once entering the zone, the motion direction of particles will be changed. The change value can be indicated by relative deflection angle. It can be seen that the deflection angles are related to particle density. When particles are impacting on the workpiece, particles with density of 2600 kg/m^3 have the relative deflection angle of 6.7°, particles with density of 4200 kg/m^3 have the relative deflection angle of 3°, and particles with density of 7850 kg/m^3 have the relative deflection angle of 1.5°. In conclusion, the deflection angles decrease with the increasing of particle density.

From Fig. 13, it can be seen that when particles are entering the flow field from the inlet, as the initial velocity of particles is 0 m/s, the velocity of the fluid is larger than particles. Particles will be accelerated. It can be seen that particles have been accelerated continually before they enter the static pressure zone. As the volume of particles is equal, the mass increases with the increasing of density, and particles with higher density will be difficult to be accelerated. Particles with density of 2600 kg/m^3 have the maximum velocity of particles of 395 m/s, particles with density of 4200 kg/m^3 have the maximum velocity of particles of 380 m/s, and particles with density of 7850 kg/m^3 have the maximum velocity of particles of 354 m/s. When entering the static pressure zone, the velocity of fluid is smaller than particles and particles have been decelerated. Particles with smaller density are decelerated more easily. When particles impact on the workpiece, particles with density of 2600 kg/m^3 have the velocity along *Y* axis of 166 m/s, particles with density of 4200 kg/m^3 have the velocity of 221 m/s, and particles with density of 7850 kg/m^3 have the velocity of 263 m/s. In conclusion, the impact velocities increase with the increasing of particle density.

It concludes that the higher density particles are more difficult to be accelerated as their mass is bigger, but they could obtain more kinetic energy from the liquid. After through the static pressure zone, they also have more velocity value. Having bigger inertia, their motion direction will be more difficult to be changed.

The impact velocities of different density particles along *Y* axis are shown in Fig. 14.

As the static pressure zone exists, the particles near the jet center will departure the jet axis with a distance and impact on

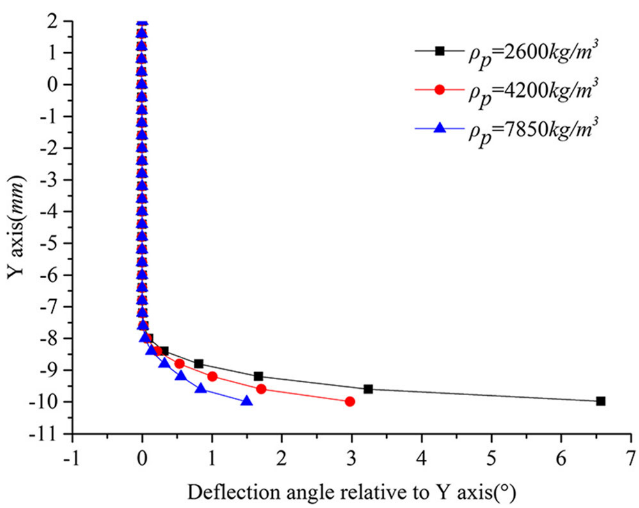

Fig. 12 Deflection angle relative to *Y* axis of particles with different densities

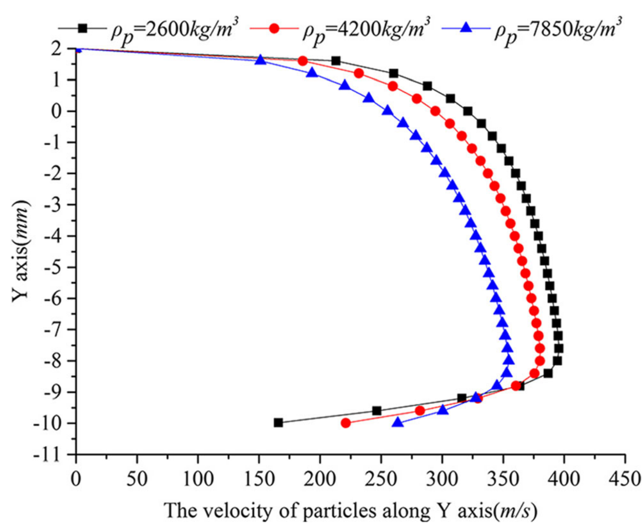

Fig. 13 The velocity along *Y* axis of particles with different densities

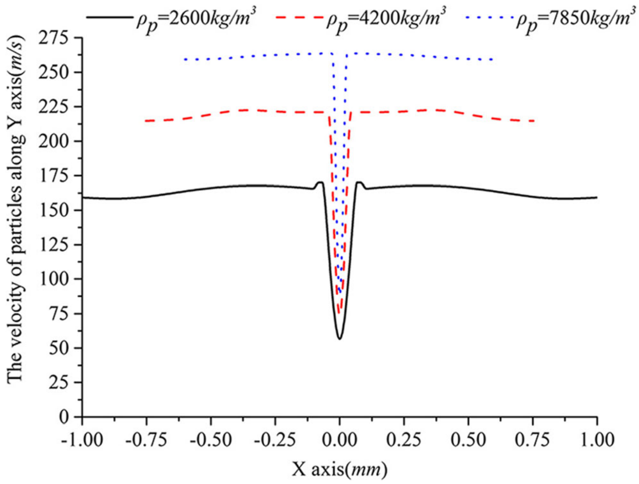

Fig. 14 The distribution of velocities of particles along Y axis on the workpiece

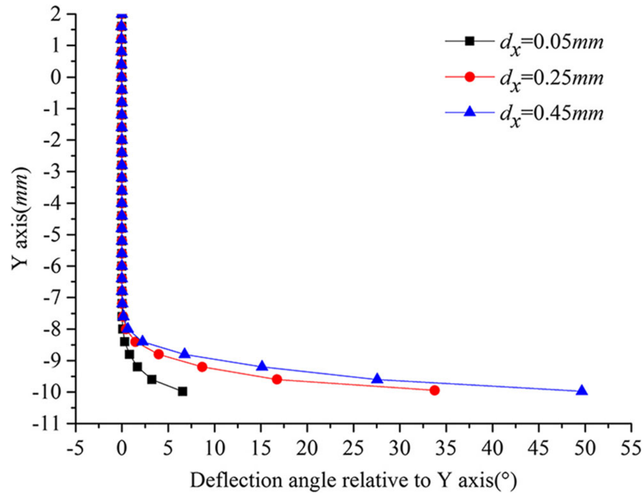

Fig. 15 Deflection angle relative to Y axis of particles with different radial positions

the workpiece with the higher velocity, as shown in Fig. 14. There are almost no particles that can penetrate the static pressure zone and impact on the very center of the static pressure zone. But it can be seen that the diameter of the no impact zone is very small, so the influence is not obvious in actual production. With the increasing of particle density, the diameter of the no impact zone decreases, the impact scope decreases, and the impact velocities increase. It can be concluded that particles of higher density will have higher impact velocity, and the machining zone will be more concentrated.

4.2.3 The influence of radial position

The pressure and velocity of the static pressure zone appear normal distribution; thus, abrasive particles in different radial positions will show different motion characteristics when they penetrate through the zone. The results of the influence of the radical position are obtained by CFD, when the jet pressure is 100 MPa, the diameter of particles is 180 μm, and the density is 2600 kg/m^3. The data are compared when the distance from the jet axis (d_x) is 0.05, 0.25, and 0.45 mm, as shown in Figs. 15 and 16.

From Figs. 15 and 16, it can be seen that all the particles are moving along the Y axis before they enter the static pressure zone. Particles have basically the same velocities along Y axis for the d_x which are 0.05 and 0.25 mm. The distance from the jet axis of 0.45 mm is the gas and liquid phase interaction zone. So the liquid velocity is low, and the kinetic energy which particles obtain from the liquid is small. Once entering the static pressure zone, particles will be offset by the force along X axis which is caused by the zone. With the increasing of d_x, the difference of the force along X axis on both sides of particles is increasing, so their deflection angles are greater.

According to Figs. 10 and 14, it can be seen that the velocities of particles in different radial positions are related to the diameter and density of particles. And the velocities tend to be the same with the increasing of diameter and density. That is to say using the greater diameter or higher density will make the material removal rates become uniform in the machining zone.

5 Conclusions

CFD simulations of the influence on the motion characteristics of particles with different process parameters have been presented. The results can be concluded as follows:

(1) Finite element simulation results show that the static pressure zone exists in the flow field, and the velocity and pressure characteristics of the static pressure zone

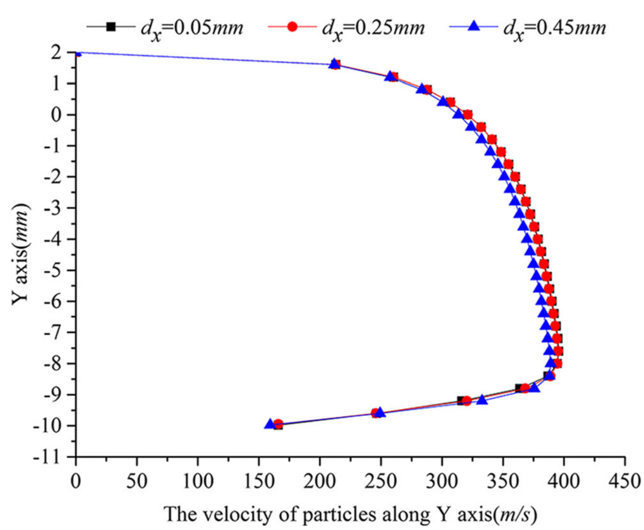

Fig. 16 The velocity along Y axis of particles with different radial positions

are analyzed. The results show that the pressure is very high and the velocity is almost zero at the center of this zone.

(2) Under the condition that jet pressure and abrasive particle density are of certain values, the results are obtained by changing the particle diameter. It shows that the deflection angle decreases and the impact velocity increases with the increasing of the diameter particle, when the particles are penetrating through the static pressure zone.

(3) Under the condition that jet pressure and the particle diameter are of certain values, the results are obtained by changing the particle density, and it shows that the impact velocity increases and the deflection angle decreases with the increasing of particle density.

(4) Under the condition that jet pressure, particle density, and particle diameter are of certain values, the results are obtained by changing the radial distance from the jet axis. It shows that the particle velocity near the jet center will be higher, and the relative deflection angle increases with the radial distance increasing.

In conclusion, using the greater diameter or higher density particles can make the particle velocity in the cross section approaching the same, and abrasive water jet can realize more uniform descaling and can increase the descaling efficiency. Reducing the diameter of abrasive particles can increase the surface roughness. But too small particles have been proven not suitable, as the impact velocity is too small and the relative deflection angle is too great. So the abrasive particles play important roles on the descaling quality and efficiency. The results have good guiding significance for abrasive particle choice.

Acknowledgments This work was supported by the Natural Science Foundation of Shanxi Province, China (No. 201601D011052).

References

1. Babu MK, Chetty OVK (2002) Studies on recharging of abrasives in abrasive water jet machining. Int J Adv Manuf Technol 19(9): 697–703
2. Abreu e Lima CE, Lebrón R, de Souza AJ, Ferreira NF, Neis PD (2016) Study of influence of traverse speed and abrasive mass flowrate in abrasive water jet machining of gemstones. Int J Adv Manuf Technol 83:77–87
3. Kevin V, Alan M (2008) Eco-pickled surface: an environmentally advantageous alternative to conventional acid pickling. Iron & Technology 5(8):81–96.1
4. Wang XC, Mao ZW, Yang Q (2012) Research on high pressure abrasive water jet for cold rolling descaling. Adv Mater Res 572: 31–36.1
5. MOMBER ANDREASW, KOVACEVIC RADOVAN (2000) Particle size distribution influence in high speed erosion of aluminium. Particulate Science & Technology 18(3):199–212
6. Labus TJ, Neusen KF, Alberts DG, Gores TJ (1991) Factors influencing the particle size distribution in an abrasive waterjet. Journal of Manufacturing Science & Engineering 113(4):402–411
7. Momber A., Pfeiffer D., Kovacevic R, Schunemann R. (1996) The influence of abrasive grain size distribution parameters on the abrasive water jet machining process. Proceedings of the 1996 24th NAMR1 conference, Society of Manufacturing Engineers MR96(115), p 1–6
8. Krishnaiah Chetty OV, Ramesh Babu N (1999) Some investigations on abrasives in abrasives waterjet machining. Proceeding of 10th American waterjet conference, Waterjet Technology Association, USA, p 419–430
9. Kantha Babu M, Krishnalah Chetty OV (2001) Studies on the use of local abrasives in abrasive waterjet machining. Proceedings of 17th International conference on CAD/CAM, Robotics and Factories of Future, Durban, South Africa, p 150–156
10. Guo N, Louis H, Meier G, Ohlsen J (1992) Recycling capacity of abrasives in abrasive water jet cutting. Proceedings of 1lth International conference on Jet Cutting Technology, Scotland, p 503–523
11. Aydin G (2014) Recycling of abrasives in abrasive water jet cutting with different types of granite. Arab J Geosci 7(10):4425–4435
12. Babu MK, Chetty OVK (2003) A study on recycling of abrasives in abrasive water jet machining. Wear 254(7–8):763–773
13. Dong Y, Liu W, Zhang H, Zhang H (2014) On-line recycling of abrasives in abrasive water jet cleaning. Procedia Cirp 15:278–282
14. Aydin G, Karakurt I, Aydiner K (2011) An investigation on surface roughness of granite machined by abrasive waterjet. Bull Mater Sci 34(4):985–992
15. Liu H, Wang J, Kelson N, Brown RJ (2004) A study of abrasive waterjet characteristics by CFD simulation. J Mater Process Technol 153(1):488–493
16. Zhang C, Zhang Y, Zhang F, Luan D (2015) Study on removal model of abrasive waterjet machining. Journal of Mechanical Engineering 51(7):39–50
17. BITTER JG (1963) A study of erosion phenomena: part I. Wear 6(1):5–21.1
18. BITTER JG (1963) A study of erosion phenomena: part II. Wear 6(3):169–190
19. Abdel-Fattah A (2007) Numerical and experimental study of turbulent impinging twin-jet flow. Experimental Thermal & Fluid Science 31(8):1061–1072
20. Fluent, Fluent 14.0 user guide, Fluent Inc
21. Wang RJ, Wang CY, Wen W, Wang J (2016) Experimental study on a micro-abrasive slurry jet for glass polishing. Int J Adv Manuf Technol:1–12
22. Li Z, Li S, Dai Y, Peng X (2010) Optimization and application of influence function in abrasive jet polishing. Appl Opt 49(15):2947–2953
23. Finnie I (1960) Erosion of surfaces by solid particles. Wear 3(2):87–103
24. Liu D, Zhu H, Huang C, Wang J, Yao P (2016) Prediction model of depth of penetration for alumina ceramics turned by abrasive waterjet—finite element method and experimental study. Int J Adv Manuf Technol:1–10